Analysis of suction induced hang-up in an ore pass

T. Vo & A.R. Russell
Centre for Infrastructure Engineering and Safety, School of Civil and Environmental Engineering, The University of New South Wales, Sydney, NSW, Australia, 2052

H. Yang
Formerly at The University of New South Wales

ABSTRACT: This paper addresses the problem of ore hang-up in a mine. A hang-up in a plane ore pass is analysed using the methods of discontinuous stress and velocity fields. The system consisting of broken ore material and a stiff ore pass wall is idealised as a plastic-rigid continuum satisfying the Mohr-Coulomb failure criterion and an associated flow rule. The influence of moisture in the ore, and its associated suction, is accounted for using the effective stress concept for unsaturated geomaterials. A simple failure mechanism consisting of three rigid blocks is assumed which is consistent with a bursting failure type and with the existence of a compressive arch underneath the hang-up section. Stress equilibrium and kinematic restrictions enable the derivation of simple algebraic expressions governing the stability of a hang-up. The separate influences of suction and cohesion are evident in the derived expressions. It is shown how the ore pass size for hang-up instability is strongly dependant on moisture content and suction. An increase in suction increases the minimum ore pass dimension needed to avoid hang-up formation.

1 INTRODUCTION

The phenomenon of hang-up in an ore pass is of interest to underground mine operators as it may lead to loss of productivity and a heavy financial cost to clear them. There are two types of hang-up. One type is governed by the ratio D/d, where D is the ore pass width and d is a characteristic dimension of the ore, usually the size of the largest ore fragments, and is referred to as an interlocking hang-up (Hadjigeorgiou & Lessard 2010; Jenike 1961; Kvapil 1965). The other type forms as a result of sticky, fine particles adhering to each other and the ore pass wall and depends primarily on the cohesion of the ore material and its moisture content (Hambley 1987). Ore materials generally contain particles ranging in size from one or two meters to just a few micro-meters in diameter. Ore segregates during handling, tipping and flow through an ore pass. It is the fine component of the ore material which builds up on the ore pass walls and causes hang-up (Fig. 1). This is exacerbated by moisture in the fine component as the moisture induces a suction increasing its strength and the possibility of hang-up formation. Suction and cohesion induced hang-ups are problematic. They are more difficult to dislodge with explosives than interlocking hang-ups (Hadjigeorgiou et al. 2005). There is also a risk of mud rushes (Butcher et al. 2005) when water is introduced to lower suction and release the hang-up.

There have been related studies on a range of blockage and arching problems in ore passes and hoppers. Amongst the first were Jenike (1961) and Kvapil (1965) which involved small scale experiments focussing on blockage at narrow discharge zones. Others involved analytical and numerical work (Arnold & McLean 1976a, 1976b; Drescher 1991; Enstad 1975; Jenike 1961; Mróz & Drescher 1969; Pariseau & Pfleider 1968; Walker 1966) and experiments (Drescher et al. 1995a, 1995b; Guo et al. 2014). However, hang-ups are formed by different mechanisms to blockages (Hadjigeorgiou & Lessard 2007) as they develop in the flowing zone where the ore pass is wider and approximately constant. Research has used empirical and numerical methods to study the influences of ore pass geometry and ore properties on the frequency of hang-ups (Esmaieli 2010; Hadjigeorgiou & Lessard 2007; Holl & Fairon 1973), but there has been no mechanistic analyses of the hang-up problem. This paper addresses this knowledge gap.

In this paper the hang-up problem is solved analytically using the methods of discontinuous stress and velocity fields. They are suitable for the ore hang-up problem because the system consisting of broken ore material passing through a stiff walled ore pass can be idealised as a plastic-rigid continuum. This greatly simplifies analysis. The versatility of the analysis is demonstrated by adapting a simple hang-up failure mechanism to plane vertical and inclined ore passes.

Critical to the stability of an arch, and therefore hang-up, are the cohesion of the ore material and its moisture content. The paper includes a suction influence (which exists when the ore is moist) in addition to a cohesion influence in the governing mechanics. It is demonstrated how suction can be used in a definition of the effective stress and shear strength and then appear in the governing equations.

Figure 1. The photograph shows the inside of an ore pass (looking down) once a hang-up had been dislodged by intervention. The remains of the sticky, fine particles which adhered to the ore pass wall are clearly visible. The ore pass is circular in section with a diameter of 2.8 m and its inclined at 70° above the horizontal. The ore contains particles as large as 1.2 m, although larger particles do not adhere to the ore pass wall so they are not present in the photo.

2 ANALYSIS

2.1 *Effective stress and shear strength for unsaturated geomaterials*

An effective stress for saturated soils was defined by Terzaghi (1936) as:

$$\sigma' = \sigma - u_{\mathrm{w}} \tag{1}$$

where, $\sigma' \equiv$ effective stress; $\sigma \equiv$ total stress and $u_w \equiv$ pore water pressure. For unsaturated soils and other geomaterials, Bishop (1959) proposed an extension of Terzaghi's effective stress as:

$$\sigma' = (\sigma - u_{\mathrm{a}}) + \chi(u_{\mathrm{a}} - u_{\mathrm{w}}) = \sigma_{\mathrm{net}} + \chi s \tag{2}$$

where, $u_{\mathrm{a}} \equiv$ pore air pressure; $\chi \equiv$ effective stress parameter; $\sigma - u_{\mathrm{a}} = \sigma_{\mathrm{net}} \equiv$ net stress (i.e. total stress in excess of pore air pressure) and $u_{\mathrm{a}} - u_{\mathrm{w}} = s \equiv$ suction. Bishop (1960) suggested that χ depends on many factors including degree of saturation (S_r), s, whether the material is undergoing drying or wetting and stress history. χ attains a value of 1 for saturated conditions and 0 for dry conditions. A prime indicates that the stress is effective.

For simplicity it is assumed that the ore's strength can be defined by the Mohr-Coulomb failure criterion, in which friction angle (φ') and cohesion (c') are independent of s, meaning the same values apply to saturated, dry and unsaturated conditions. There is experimental evidence showing this to be a reasonable approximation (Escario 1980; Gan et al. 1988; Likos 2010). The shear strength (τ) is then:

$$\tau = c' + \sigma' \tan\varphi' = c' + (\sigma_{\mathrm{net}} + \chi s)\tan\varphi' \tag{3}$$

For simplicity it is also assumed that the product χs, representing the contribution of suction to the effective stress, is constant.

2.2 *Work dissipated in a hang-up section*

To calculate the work dissipated in a hang-up section, a dissipation function must be defined. It is assumed in this paper that the ore material is unsaturated and obeys the associated flow rule. An increment of work dissipated per unit length of velocity discontinuity for a unit width can be found by a procedure similar to Davis (1968) and Atkinson (2014). At a velocity discontinuity an increment of internal work dissipated (δW_{int}) is given by:

$$\delta W_{\mathrm{int}} = \tau \delta d_{\mathrm{t}} + \sigma \delta d_{\mathrm{n}} \tag{4}$$

where, $\delta d_{\mathrm{t}} \equiv$ displacement increment tangential to a velocity discontinuity and $\delta d_{\mathrm{n}} \equiv$ displacement increment normal to a velocity discontinuity. Equation 4 is valid for a constant χs condition (with no associated work) and for a plane problem because the quantities δd_{t} and δd_{n} are conjugate to the quantities τ and σ. Substituting $\delta d_{\mathrm{t}} = -\delta d_{\mathrm{n}}/\tan\psi$ and Equation 3 into Equation 4, assuming atmospheric air pressure and evoking the associated flow rule to obtain:

$$\delta W_{\mathrm{int}} = (\chi s \sin\varphi' + c' \cos\varphi')\delta d_{\mathrm{max}} \tag{5}$$

where, $\delta d_{\mathrm{max}} \equiv$ total displacement increment at the velocity discontinuity. It is accepted that the associated flow assumption here is highly idealised at the interface between a hang-up and an ore pass wall, particularly when their mineralogy is significantly different. When $\chi s = 0$, Eq. 5 reduces to the usual expression $\delta W_{\mathrm{int}} = (c' \cos\varphi')\delta d_{\mathrm{max}}$ for dry geomaterials. Equation 5 is used for all calculations involving internal work dissipation in this paper.

2.3 *Investigation of the ore pass hang-up problem by discontinuous stress and velocity fields*

In this section, it is assumed that a compressive arch is formed underneath a hang-up section and the normal stress on the arch surface is zero. A pressure q_{s} is assumed to act perpendicular to the surface of the hang-up section in the direction of gravity. The limit load can be calculated by summing q_{s} over this surface.

The existence of an arch underneath the hang-up section requires average normal stresses to increase with height (Brown et al. 2000; Guo et al. 2014; Rotter et al. 2002). This means that to break away from static equilibrium, the arch is more likely to burst than to collapse. A bursting failure is characterised by an initial upward movement of the ore material in a hang-up section. A trigger of a bursting failure may be a mechanical impact or blast. For a bursting failure mechanism, the limit loads calculated from a discontinuous stress field are larger than the limit loads calculated from a discontinuous velocity field. In the presentation that follows the limit surcharge load (q_s) features in the normalised pressure ratio $q_s/(\chi s + c' \cot \varphi')$.

2.3.1 *Hang-up in a plane vertical ore pass: the bursting mechanism*

The geometry of a hang-up in a plane vertical ore pass section is shown in Figure 2a. The arch underneath the hang-up is idealised in that it is bounded by two linear segments. It is assumed in Figure 2a that the in-plane dimension is infinitely long. As the section is symmetric the displacement increment diagram for only half of it is shown in Figure 2b.

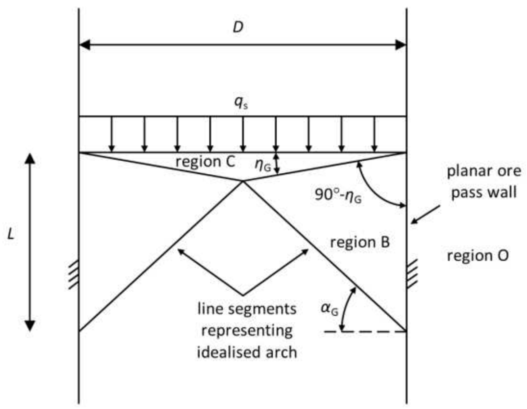

a. Geometry showing different regions.

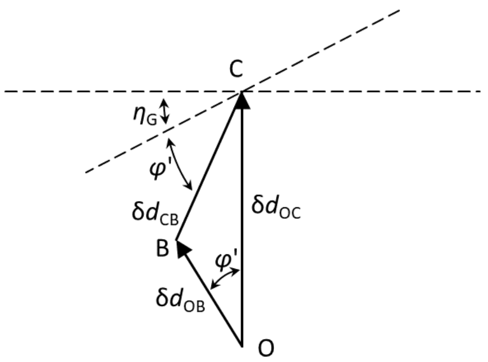

b. Displacement increment diagram.

Figure 2. A plane vertical ore pass.

Equating the sum of external work inputs (δW_{ext}) due to gravity and surcharge to the sum of internal works (δW_{int}) dissipated at velocity discontinuities OB and BC to obtain:

$$\frac{q_s}{\chi s + c' \cot \varphi'} + \frac{\gamma}{\chi s + c' \cot \varphi'} \left(\frac{D \tan \eta_G}{4} + \frac{L \cos \varphi'}{2} \frac{\delta d_{OB}}{\delta d_{OC}} \right) = -\sin\varphi' \left(\frac{2L}{D} \frac{\delta d_{OB}}{\delta d_{OC}} + \frac{1}{\cos \eta_G} \frac{\delta d_{CB}}{\delta d_{OC}} \right) \quad (6)$$

Equation 6 shows that q_s is a function of weight and ore pass geometry. The influence of ore pass geometry on q_s can be separated from the influence of weight. The influence of ore pass geometry on q_s is revealed by putting $\gamma = 0$ in Equation 6 so it becomes:

$$\frac{q_s}{\chi s + c' \cot \varphi'} = -\sin\varphi' \left(\frac{2L}{D} \frac{\delta d_{OB}}{\delta d_{OC}} + \frac{1}{\cos \eta_G} \frac{\delta d_{CB}}{\delta d_{OC}} \right) \quad (7)$$

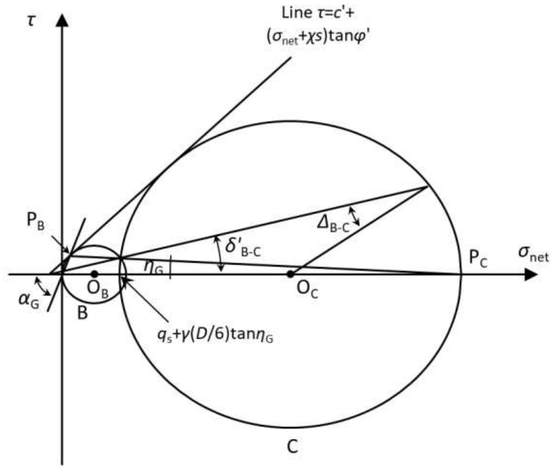

a. Vertical stress is the minor principal stress in zone C.

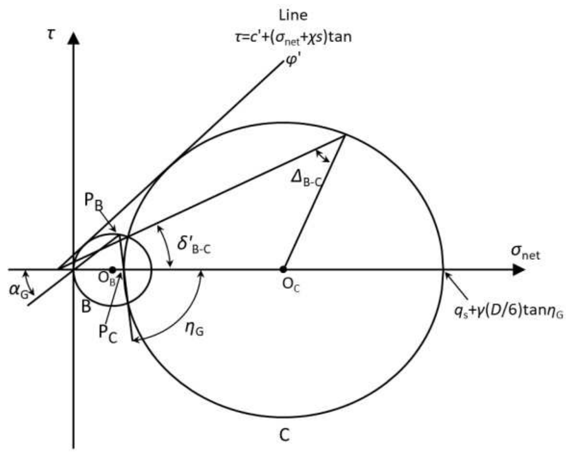

b. Vertical stress is the major principal stress in zone C.

Figure 3. Mohr's circle plot showing stress discontinuities and stress states.

Figures 3a and 3b show the stress states of regions B and C on Mohr's circle plots for two statically admissible mechanisms. For one mechanism the vertical stress is the minor principal stress in region C (Fig. 3a). For the other mechanism the vertical stress is the major principal stress (Fig. 3b). The pole point P_C is located on the horizontal axis so that the shear stress on the axis of symmetry is zero.

With reference to Figures 3a and 4a, the following relation is obtained:

$$\frac{q_s+\gamma(D/6)\tan\eta_G}{\chi s+c'\cot\varphi'}=\frac{\sin\varphi'}{1-\sin\varphi'}\left[1+\frac{\sin(180°-2\Delta_{B-C})}{\sin(\Delta_{B-C}-\delta'_{B-C})}\right]-$$

$$\sin\varphi'\left[1+\frac{\sin\varphi'}{1-\sin\varphi'}+\frac{\sin(180°-2\Delta_{B-C})}{\sin(\Delta_{B-C}-\delta'_{B-C})}\frac{\sin\varphi'}{1-\sin\varphi'}\right] \quad (8)$$

With reference to Figures 3a and 4b, the following relation is obtained:

$$\frac{q_s+\gamma(D/6)\tan\eta_G}{\chi s+c'\cot\varphi'}=\frac{\sin\varphi'}{1-\sin\varphi'}\left[1+\frac{\sin(180°-2\Delta_{B-C})}{\sin(\Delta_{B-C}-\delta'_{B-C})}\right]+$$

$$\sin\varphi'\left[1+\frac{\sin\varphi'}{1-\sin\varphi'}+\frac{\sin(180°-2\Delta_{B-C})}{\sin(\Delta_{B-C}-\delta'_{B-C})}\frac{\sin\varphi'}{1-\sin\varphi'}\right] \quad (9)$$

Since the right-hand side of Equation 8 is smaller than that of Equation 9, the mechanism shown in Figure 3a is more critical than Figure 3b.

For the case when the ore self-weight is neglected ($\gamma = 0$) the influence of ore pass geometry on the stability of a hang-up section is studied. Figures 4a and 4b show that the stress and velocity solutions bound regions containing the exact limit loads. This region is defined as (and denoted in Figures 4a and 4b) a region of possible instability. This means that for a given value of α_G there exists a range of $q_s/(\chi s + c'\cot\varphi')$ where a hang-up is potentially unstable. Outside this region a hang-up is stable.

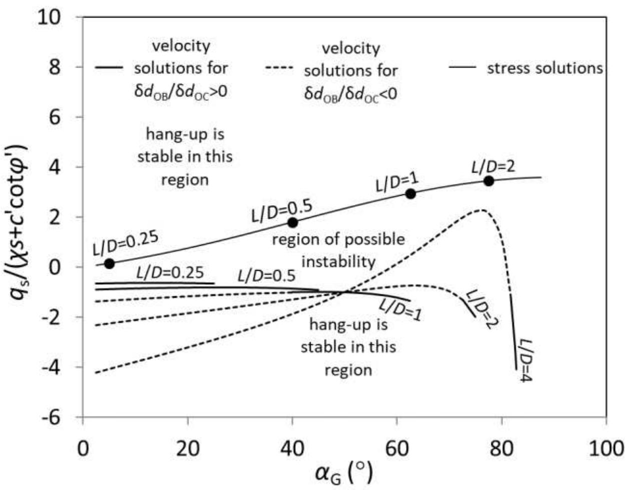

Figure 4. Comparison of discontinuous stress and velocity solutions for a bursting failure mechanism in plane vertical ore pass for when $\varphi' = 40°$.

2.3.2 *Hang-up in a plane inclined ore pass*

The geometry of a hang-up in a plane inclined ore pass is shown in Figure 5a. When the influence of ore self-weight is neglected ($\gamma = 0$), the influence of ore pass geometry on the stability of hang-up can be studied from discontinuous stress and velocity solutions. Figure 5b shows the influence for $\varphi' = 40°$. The discontinuous velocity solutions are plotted for $L/D = 0.5$ and $u = v$ (Fig. 5a). For clarity, only admissible discontinuous velocity solutions are shown. The discontinuous stress solutions are plotted for an inclined ore pass for two cases. In one case, L/D=constant (the thick dashed curves in Fig. 5b). In the other case, δ'_{B-C}=constant (the thin dashed curves in Fig. 5b). Figure 5b shows that in both cases the discontinuous stress solutions increase as β_G reduces from 90° i.e. the assumed bursting failure mechanism is less likely to occur in an inclined ore pass than in a vertical ore pass. Figure 5b shows that the discontinuous velocity solutions at $\beta_G = 75°$ are close to the discontinuous velocity solutions at $\beta_G = 90°$ but at $\beta_G = 30°$ they are significantly smaller than the discontinuous velocity solutions at $\beta_G = 90°$. This indicates that the assumed bursting mechanism is less likely to occur in an ore pass inclined at $\beta_G = 30°$ than in a vertical ore pass.

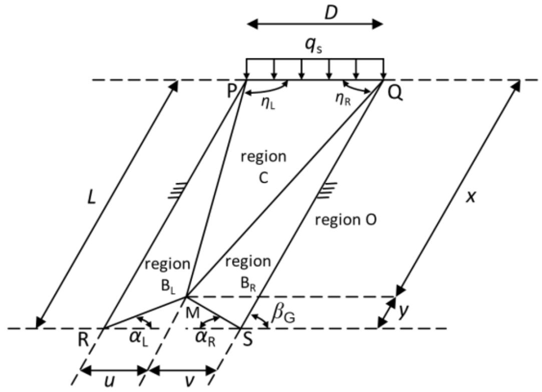

a. The geometry of a hang-up in a plane inclined ore pass.

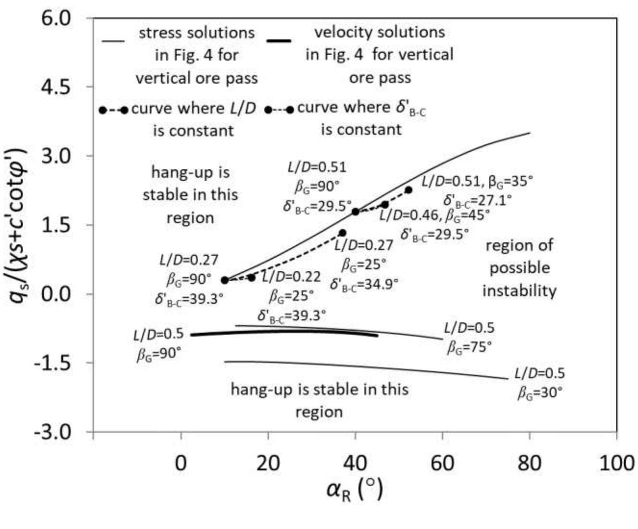

b. Discontinuous stress solutions and discontinuous velocity solutions for when $\varphi' = 40$.

Figure 5. Influence of ore pass inclination angle on discontinuous stress and discontinuous velocity solutions for when $\varphi' = 40$.

3 ASSESSING HANG-UP STABILITY

When the width to length ratio of an ore pass is approximately zero (i.e. L/D is large), Hambley

(1987) suggested a design criterion to prevent cohesive hang-ups of the form:

$$D > \frac{c'}{\gamma} A_0 \tag{10}$$

where, $A_0 = 6(1 + \sin\varphi')$.

In Section 2, the method of stress discontinuity was used to find a condition separating a stable hang-up from a potentially unstable hang-up. In a vertical ore pass, for non-zero values of γ and q_s, the critical condition is expressed by Equation 8, which can be written in an alternate form:

$$\frac{q_s + \gamma(D/6)\tan\eta_G}{\chi s + c'\cot\varphi'} = \frac{\sin\varphi' \sin 2\alpha_G}{\sin 2\eta_G} \tag{11}$$

It follows, for $q_s = 0$, that the required D to cause potential instability for a given χs, φ', c' and γ is:

$$D > \left(\frac{\chi s + c'\cot\varphi'}{\gamma}\right) A_1 \tag{12}$$

where, $A_1 = \frac{3\sin\varphi' \sin 2\alpha_G}{(\sin\eta_G)^2}$.

Equation 12 can be made closer to the exact value by minimising the quantity A_1 subject to $\alpha_G \geq \eta_G$ (as $\alpha_G \geq \eta_G$ is essential for the validity of the problem geometry used in the derivation). The quantity A_1 becomes smallest when $\alpha_G = \eta_G$ so the criterion in Equation 12 becomes:

$$D > \left(\frac{\chi s + c'\cot\varphi'}{\gamma}\right) \min\{A_1\} =$$

$$\left(\frac{\chi s + c'\cot\varphi'}{\gamma}\right) \frac{6\sin\varphi' \cos\alpha_G}{\sin\eta_G} \tag{13}$$

Examples are now given to illustrate how the criterion given by Equation 13 can be applied using strengths and suctions for a typical ore (Vo et al. 2016).

In the first example the peak strength of the ore material ($c' = c'_p = 10$ kPa and $\varphi' = \varphi'_p = 57.4°$) is assumed to prevail at the onset of instability. It is assumed that $e = 0.22$, $\rho_d = 2600$ kg/m^3 and $\gamma = 25.48$ KN/m^3. It is required to estimate D to make hang-up instability possible for different χs. Substituting these properties into Equation 13 gives:

$$D > \left(\frac{\chi s + 6.40}{25.48}\right) 24.97 \text{ (m)} \tag{14}$$

For dry conditions, $\chi s = 0$ and Equation 14 gives $D >$ 6.3 m. For the ore at a moisture content (ω) = 2.5 % (when $\chi s =$ 6.81 kPa) $D >$ 12.9 m. For the ore at ω = 5 % (when $\chi s =$ 3.60 kPa) $D >$ 9.8 m. It is noted that for dry conditions (i.e. $\chi s =$ 0), Hambley's solution gives $D >$ 4.2 m, compared to $D >$ 6.3 m from the new solution presented here.

In the second example the softened strength ($c' = c'_s = 0$ kPa and $\varphi' = \varphi'_s = 49.6°$) is assumed to prevail at the onset of instability. Substituting these properties into Equation 13 gives:

$$D > \left(\frac{\chi s}{25.48}\right) 18.46 \text{ (m)} \tag{15}$$

For dry conditions, $\chi s = 0$ so $D >$ 0 m meaning hang-up would not occur. For ω = 2.5 %, $\chi s =$ 6.8 kPa and $D >$ 4.9 m. For ω = 5 %, $\chi s =$ 3.60 kPa and $D >$ 2.6 m.

The examples given show a significant effect of ω (through χs) on the D needed for possible hang-up instability. If peak strengths are used, a 2.5 % moisture content requires D to be more than double that of dry conditions. However, a 5 % moisture content requires D to be only 1.6 times that of dry conditions. It is evident that there is a diminishing effect with increasing ω, since D reduces as ω increases.

The strength used also has a significant influence on D needed for possible hang-up instability. At ω = 2.5 % and ω = 5 % the softened strength requires $D >$ 4.9 m and $D >$ 2.6 m, respectively. These are much different from the requirements $D >$ 12.9 m and $D >$ 6.3 m, respectively, calculated when peak strength is used.

The criterion in Equation 13 was derived assuming a plane vertical ore pass. It was shown that the potential for hang-up instability does not differ significantly between vertical ($\beta_G = 90°$) and near vertical ($\beta_G >$ about 65°) ore passes. (β_G is the angle above the horizontal). The potential for hang-up instability drastically reduces for ore passes inclined at $\beta_G < 45°$. Consequently, the criterion in Equation 13 should not be used when ore passes are not vertical or near vertical. Also, other complex aspects of ore pass design, such as the effects of shape and dimension, need further investigation.

4 CONCLUSION

A new criterion for cohesion and suction induced hang-up was presented for plane and inclined ore passes. It was derived using the methods of stress and velocity discontinuities. A hang-up was assumed to consist of three rigid blocks. In the method of stress discontinuity, the rigid blocks satisfy equilibrium and the Mohr-Coulomb failure criterion. In the method of velocity discontinuity, the rigid blocks were assumed to undergo small displacements consistent with a bursting failure. The displacement increments satisfied the associated flow rule and kinematic restrictions at the boundaries.

The influences of suction were incorporated using the effective stress concept for unsaturated geomaterials. The contributions of suction to effective stress, χs, and strength properties were assumed constant. A simple function was used to calculate the internal work dissipated and it is valid for plane analyses. The function enabled stress solutions to be linked to the velocity solutions.

The analysis showed a significant influence of the ratio L/D on the stability of a hang-up.

For dry ore materials the new criterion was compared to that of Hambley (1987). For a set of typical ore properties, the new criterion specifies that the ore pass width D to cause potential instability must be at least 6.3 m, 1.45 times the value using the criterion of Hambley (1987). Also, it was shown that a 2.5 % moisture content increases the minimum D to 12.9 m, more than double the dry value. For softened strength parameters and a 2.5 % moisture content the new criterion specifies that D must be at least 4.9 m. The effect of moisture on D was significant.

5 REFERENCES

Arnold, P.C. & McLean, A.G. 1976a. An analytical solution for the stress function at the wall of a converging channel. *Powder Technology* 13: 255-260.

Arnold, P.C. & McLean, A.G. 1976b. Improved analytical flowfactors for mass-flow hoppers. *Powder Technology* 15: 279-281.

Atkinson, J.H. 2014. *The Mechanics of Soils and Foundations* (2nd ed.): Taylor and Francis.

Bishop, A.W. 1959. The principle of effective stress. *Teknisk Ukeblad* 106(39): 859-863.

Bishop, A.W. 1960. The measurement of pore pressure in the triaxial test. In *the Proceedings of Conference on Pore Pressure and Suction in Soils*, London, UK.

Brown, C.J., Lahlouh, E.H. & Rotter, J.M. 2000. Experiments on a square planform steel silo. *Chemical Engineering Science* 55: 4399-4413.

Butcher, R., Stacey, T.R. & Joughin, W.C. 2005. Mud rushes and methods of combating them. *Journal of the South African Institute of Mining and Metallurgy* 105(11): 817-824.

Davis, E.H. (Ed.) 1968. *Theories of soil plasticity and the failure of soil masses*. London: Butterworths.

Drescher, A. 1991. *Analytical Methods in Bin-Load Analysis*. Amsterdam: Elsevier.

Drescher, A., Waters, A.J. & Rhoades, C.A. 1995a. Arching in hoppers: I. arching theories and bulk material flow properties. *Powder Technology* 84: 165-176.

Drescher, A., Waters, A.J. & Rhoades, C.A. 1995b. Arching in hoppers: II. arching theories and critical outlet size. *Powder Technology* 84: 177-183.

Enstad, G. 1975. On the theory of arching in mass-flow hoppers. *Chemical Engineering Science* 30: 1273-1283.

Escario, V. 1980. Suction-controlled penetration and shear shear tests. In *the The Fourth International Conference on Expansive Soils*, Denver, Colorado.

Esmaieli, K. 2010. *Stability analysis of ore pass systems at Brunswick mine.* (PhD), Université Laval, Québec.

Gan, J.K.M., Fredlund, D. & Rahardjo, H. 1988. Determination of the shear strength parameters of unsaturated soil using the direct shear test. *Canadian Geotechnical Journal* 25(3): 500-510.

Guo, J., Roberts, A.W. & Prigge, J.D. 2014. Experimental investigation of wall pressure and arching behaviour under surcharge pressure in mass-flow hoppers. *Powder Technology* 258: 272-284.

Hadjigeorgiou, J. & Lessard, J.F. 2007. Numerical investigations of ore pass hang-up phenomena. *International Journal of Rock Mechanics and Mining Sciences* 44(6): 820-834.

Hadjigeorgiou, J. & Lessard, J.F. 2010. Strategies for restoring material flow ini ore and waste pass systems. *International Journal of Mining, Reclamation and Environment* 24(3): 267-282.

Hadjigeorgiou, J., Lessard, J.F. & Mercier-Langevin, F. 2005. Ore pass practice in Canadian mines. *Journal of the South African Institute of Mining and Metallurgy* 105: 809-816.

Hambley, D.F. 1987. Design of ore pass systems for underground mines. *CIM Bulletin* 897: 25-30.

Holl, G.W. & Fairon, E.G. 1973. A review of some aspects of shaft design. *Journal of the South African Institute of Mining and Metallurgy* 73: 309-324.

Jenike, A.W. 1961. *Gravity flow of bulk solids* (Bulletin No. 108). Retrieved from Salt Lake, USA.

Kvapil, R. 1965. Gravity flow of granular materials in hoppers and bins in mines - II. coarse material. *International Journal of Rock Mechanics and Mining Sciences* 2: 277-304.

Likos, W.J. 2010. Modified direct shear apparatus for unsaturated sands at low suction and stress. *Geotechnical Testing Journal* 33(4): 286-298.

Mróz, Z. & Drescher, A. 1969. Limit plasticity approach to some cases of flow of bulk solids. *Journal of Manufacturing Science and Engineering* 91(2): 357-364.

Pariseau, W.G. & Pfleider, E.P. 1968. Soil plasticity and the movement of materials in ore passes. *Transactions of the Society of Mining Engineers of AIME* 241(1): 42-56.

Rotter, J.M., Brown, C.J. & Lahlouh, E.H. 2002. Patterns of wall pressure on filling a square planform steel silo. *Engineering Structures* 24: 135-150.

Terzaghi, K. v. 1936. *The shearing resistance of saturated soils and the angle between the planes of shear.* In *the First International Conference on Soil Mechanics and Foundation Engineering.*

Vo, T., Yang, H. & Russell, A.R. 2016. Cohesion and suction induced hang-up in ore passes. *International Journal of Rock Mechanics and Mining Sciences* 87: 113-128.

Walker, D.M. 1966. An approximate theory for pressures and arching in hoppers. *Chemical Engineering Science* 21(11): 957-997.